Betaine ameliorates intestinal injury by targeting the LPS/TLR4/MyD88 pathway and microbial communities of intestinal tract in acute liver failure

Qian Chen
Renmin Hospital of Wuhan University
Yao Wang
Renmin Hospital of Wuhan University
Fang-Zhou Jiao
Renmin Hospital of Wuhan University
Chun-Xia Shi
Renmin Hospital of Wuhan University
Mao-Hua Pei
Renmin Hospital of Wuhan University
Lu-Wen Wang
Renmin Hospital of Wuhan Universtiy
Zuo-Jiong Gong (zjgong@163.com)
Wuhan University Renmin Hospital https://orcid.org/0000-0002-4676-5856

Research

Keywords: Betaine, acute liver failure, intestinal mucosal barrier, gut microbiota

Posted Date: November 18th, 2019

DOI: https://doi.org/10.21203/rs.2.17359/v1

Abstract

Background: A growing body of evidence revealed that the gut microbiome has a marked impact in acute liver failure (ALF). Microbes and their products will translocate into enterocoelia and enter into circulation system from the damaged intestinal lumen. It will further aggravate liver injury by enhancing the spread of inflammation, tissue damage and sepsis. Betaine is a hepatoprotective drug which has anti-inflammatory and anti-oxidant effects. Here, we evaluated the impact of betaine on gut microbiota composition in ALF animal experiment. The potential protective effect of betaine by inhibiting Toll-like receptor 4 (TLR4) responses was explored as well.

Results: Eighteen mice were randomly divided into normal, model, and betaine groups. The ALF-induced intestinal epithelial barrier disruption internal models were induced by D-galactosamine（D-Gal）and lpopolysaccharide (LPS). Betaine was administered intragastrically 1 week before exposure of D-Gal/LPS. LPS were solely applied with a rat small intestinal cell line IEC-18 to establish ALF-induced intestinal epithelial barrier disruption external model. Mice in the model group developed severe intestinal epithelial tissue injury than normal group, increased significantly in the protein levels of TLR4, MyD88, TRAF6 and TNF-a and the mRNA levels of TLR4 and MyD88, and decreased significantly in the protein and mRNA levels of (ZO)-1 and occludin. Whereas, all above indicators were improved significantly by administration of betaine than that in model. The degree of liver tissue pathological damage, liver function and serum inflammatory cytokines in betaine group were significantly reduced than that in model group. The permeability of mice intestinal epithelial and IEC-18 cell in models was improved in betaine group than models. A total of 509 Operational Taxonomic Units (OTUs) were produced from mice fecal samples according to 16s rRNA gene sequence analysis. There were 156 core microbiomes in fecal samples. There existed a total of 24 species contained 11 species at the genus level which had a significant difference between groups. The increased relative abundance of g-Enterorhabdus in the model group was detected compared with normal group. Betaine down-regulated the relative abundance of g-Enterorhabdus in model. The relative abundance of g-Bacteroides was the highest in normal group and the least in model group. The relative abundance of g-Prevotella was almost identical in normal and betaine group, and it was decreased in model group.

Conclusion: Betaine effectively improved the intestinal mucosal barrier in acute liver failure.
The mechanism was probably related to inhibit the LPS/TLR4/MyD88 signaling pathways, improved the intestinal mucosal barrier and then maintained the gut microbiota composition.

Background

Acute liver failure (ALF), characterized by massive liver necrosis associated with severe impairment of hepatic function, is an intractable and high mortality disease in clinical practice [1]. As for the pathogenesis of liver failure, the majority of scholars support the theory of ‘two-hit hypothesis’. The primary liver injure is caused directly or indirectly by various pathogen (such as hepatitis virus, ethanol, drugs and hepatotoxicants, etc). Intestinal endotoxemia, as the secondary liver injury, also plays an

important role in the occurrence and development of ALF [2]. In addition, the liver failure patients are susceptible to merge endotoxemia. It's mainly due to the damaged intestinal mucosal barrier which led to a significant quantities of endotoxin (lipopolysaccharide, LPS) produced by overgrowth of gram-negative bacteria [3].

The integrated intestinal wall barrier, mainly consist of intestinal mucosal epithelium, tight connection and intrinsic membrane under the epithelium [4]. The tight connection between epithelial cells, contains transmembrane proteins occludin, claudins, junctional adhesion molecules, as well as the cytoplasm protein (ZO)−1. They are the most imperative part of the intestinal wall barrier [5]. The intestinal mucosal permeability will be increased, when these junctions are altered [6]. There is a close relationship between the weakened intestinal mucosal immune function and damaged mucosal mechanical barrier bacterial. Both of them contribute to the endotoxin and excessive intestinal pathogens translocation [7]. Endotoxin is a LPS component which recognized as part of the outer membrane of gram-negative bacteria. Tool like receptors (TLRs), are pattern recognition receptors (pattern recognition receptor, PRR). They play an important role in intestinal mucosal immune system via mediating signal transduction. Particularly, TLR4-mediated recognition of LPS occurs in the formation of a receptor multimer composed of two copies of the TLR4-MD2-LPS complex. And then the complex recruits the TIR domain−containing adaptors TIRAP (Mal) and MyD88 (MyD88-dependent pathway). Once MyD88-dependent pathway is activated, the downstream signaling molecules is further activated, which lead to release a lot of inflammatory mediators such as TNF-α, IL−1β and IL−18 [8–10]. The previous study has indicated that the transcription of TLR4 is enhanced in ALF mice [11].

Increased evidences have been shown a close correlation between the gut microbiome and liver disease [12]. The liver possesses immune surveillance against multifarious pathogens which from the gut, as well as intestinal mucosal immunity and the intestinal microbiome also affect liver function [13]. The mutual effect between the gut and the liver is regared as "gut-liver axis". The integrity of the intestinal epithelial barrier has been demonstrated to be regulated by gut microbiota [14]. A compromised intestinal mucosal barrier contributes the bacteria translocation into portal vein and then reach to the liver. It leads more inflammation, liver cell apoptosis, and rapid progression to multiple organ failure [15]. The pathogenic *Proteus* is increasing in ALF rats and markedly depleting the *Coriobacteriaceae, Bacteroidales* and *Allobaculum* in ALF rats [16]. Accumulating evidences point to gut microbiota being involved in this process. Moreover, the *Bacteroidetes, Ruminococcaceae, Porphyromonadaceae* and *Lachnospiraceae* are decreased in fecal microbial communities in acute-on-chronic liver failure (ACLF) patients compared to the levels before disease onset [17]. Besides, the levels of *Firmicutes* are ascended in ACLF patients fecal. The regulation of the intestinal microecology by microbial ecological agents has been proposed as an emerging therapeutic strategy for liver failure as well [18].

Betaine, as an essential human nutrient, exists in many tissue and organs, which are especially abundant in liver and kidney. It participates in methyl cycle. It is often used as feed additives to replace the biological function of methionine, to reduce the cost of feedstuffs [19]. Many studies have shown that betaine has many pharmacological functions such as antioxidant and anti-inflammatory effects [20, 21].

The retrospective study suggests that higher betaine intakes may be associated with a lower risk of primary liver cancer [22]. There is a favorable relationship between the blood betaine concentration and the severity of non-alcoholic fatty liver disease (NAFLD) in the community-based participants [23]. And our previous study have also indicated that betaine effectively prevents alcohol-induced and high-fat-diet-induced liver injury from inhibition of the expression of TLR4 [24, 25]. However, the effects of betaine on acute liver failure and related mechanisms are still unknown. Especially, the influence of betaine on the gut microbial ecosystem need further to study.

At present, the application of high-throughput next generation sequencing techniques allowed us to characterize the overall structure of the complex gut microbial ecosystem at the OUT level. In this study, we employed the D-Gal/ LPS in vivo and LPS in vitro to establish ALF-induced intestinal epithelial barrier disruption internal and external models respectively. Betaine was employed as an intervention agent. The relationship between the expression of key molecules in intestinal TLR4-mediated signaling pathway and intestinal tight connection protein were examined. The gut microbial ecosystem was also studied to explore potential therapeutic effect of betaine in acute liver failure.

Results

Betaine ameliorated the liver damage and improved liver function and serum inflammatory mediators in ALF mice

ALF mice model was successfully established. The liver pathological changes and serum biochemical indicators were evaluated. As HE staining shown in Fig. 1A, the structure of liver lobules and the arrangement of liver cells in normal group was clear and neat, the necrosis of liver cells and the infiltration of inflammatory cells were not observed. On the contrary, the liver lobular structure in ALF model group was deranged, and massive hepatocyte necrosis surrounded by inflammatory cells infiltration. Compared with ALF model group, the degree of hepatocyte necrosis and inflammation was significant reduced in betaine intervention groups. As shown in Fig. 1C-E. The serum ALT, AST and TBIL in models were significantly increased than that in normal group ($P < 0.05$). Compared with the model group, the ALT, AST and TBIL levels were greatly lowered in betaine groups ($P < 0.05$). The levels of inflammatory cytokines, including TNF-α, IL-1β and IL-18 in the ALF group were significantly increased compared with normal group. They were significantly decreased in betaine group than that in ALF model group ($P <0.05$) (Fig. 1F-H).

Betaine ameliorated the small intestine damages in ALF mice

As shown in Fig. 1B, histologic analysis indicated epithelial layer in models elevated from the lamina propria and villus denuded and loss of height in small intestine with remarkable inflammatory cell infiltration. By contrast, betaine conserved almost normal architecture in small intestine. With the changes in histology, the intestinal permeability significantly increased in the model group compared with the normal group ($P < 0.05$). As shown in Fig. 3A, the intestinal permeability was dramatically improved by betaine, compared with the model group ($P < 0.05$).

Betaine inhibited TLR4/MyD88 pathway in ALF mice

The effect of betaine on the TLR4/MyD88 pathway was assessed. The protein levels of TLR4, MyD88, TRAF6 and TNF-α and the mRNA levels of TLR4 and MyD88 were significantly higher in model group than that in normal group ($P < 0.05$). Compared with model group, the protein levels of TLR4, MyD88, TRAF6 and TNF-α and the mRNA levels of TLR4 and MyD88 were significantly decreased in betaine group (Fig. 2A-C and Fig. 3C).

Betaine improved the expression of (ZO)-1 and occludin in ALF mice

As shown in Fig. 2C-D and Fig. 3D, the mRNA and protein expression of (ZO)-1 and occludin were both significantly decreased in that in model group than normal ($P < 0.05$). Compared with the model group, the expressions of (ZO)-1 and occludin were significantly elevated in betaine groups ($P < 0.05$).

Betaine suppressed the TLR4/MyD88 pathway in LPS stimulated IEC-18 cell

As shown in Fig. 2E-H, the protein levels of TLR4, MyD88, TRAF6 and TNF-a were significantly increased in model group, compared with normal group ($P < 0.05$). Compared with models, the protein levels of TLR4, MyD88, TRAF6 and TNF-a were dramatically suppressed by betaine administration ($P < 0.05$). In addition, the protein expressions of TLR4, MyD88, TRAF6 and TNF-a in medium dose in betaine group were lower than low dose betaine group. They were the most low in high dose betaine group ($P < 0.05$). The mRNA levels of TLR4 and MyD88 had a statistical difference among high dose, medium dose and low dose betaine group as well (Fig.3E, $P < 0.05$). It showed a dose-depend manner.

Betaine enhanced the expression of (ZO)-1 and occludin in LPS stimulated IEC-18 cell

As shown in Fig. 2G, 2H and Fig. 3F, the expressions of (ZO)-1 and occludin protein and mRNA were significantly lower in model group than in normal ($P < 0.05$). Compared with the model group, the expression of (ZO)-1 and occludin protein and mRNA were significantly improved in betaine intervention groups ($P < 0.05$). Moreover, the proteins and mRNA expression of (ZO)-1 and occludin in medium dose betaine group were elevated than low dose betaine group, and were the highest in high dose betaine group ($P < 0.05$). The expression improvement showed a dose-depend manner.

Betaine elevated the TEER value in LPS stimulated IEC-18 cells

As shown in Fig. 3B, the TEER value in model group was greatly decreased, compared with the normal group, ($P < 0.05$). After being intervened with betaine, the TEER value were significant elevated ($P < 0.05$). There was a statistical difference among high dose, medium dose and low dose betaine group as well ($P < 0.05$). It showed a dose-depend manner.

OTUs analysis

The OTU network analysis for fecal samples of mice provided the existence of some core OTUs and a common microbial composition among each group. A total of 509 OTUs were produced from 15 fecal samples (Additional file 1). As shown in Fig. 4A, the normal group occupied the maximum OTUs, but betaine and model group possessed similar amounts OTUs. The core microbiome which covers each fecal sample could be found based on the shared OTUs of each sample and the species represented by the OTUs. There were 156 core microbiomes in fecal samples (Additional file 2).

Alpha diversity analysis

Alpha diversity contains the observed species index, the chao1 index, the shannon index and simpson index. The observed species index indicated the actual number of OTU observed and chao1 index is used to estimate the total number of OTUs contained in a sample. Both of them indicate species richness of the sample. The simpson index and shannon index are applied to estimate the species diversity. As shown in Fig. 4B-F, the fecal bacteria of normal group had the highest level of species richness and diversity. However, the species diversities of microbiota in betaine and model group did not have notable differences.

Beta diversity analysis

Different from Alpha diversity analysis, Beta diversity analysis is appropriate to compare the differences species diversity among a pair of samples. UniFrac compares species community differences using phylogenetic evolution information. The results can be used as an index to measure Beta diversity, which has taken into account the evolutionary distance between species. UniFrac results are divided into weighted UniFrac and unweighted UniFrac. Weighted UniFrac considers the abundance of sequences, and unweighted UniFrac does not. The Beta diversity analyses include the Anosim analyses and Principal Coordinates Analysis (PCoA). Anosim analysis is a nonparametric test used to detect whether the difference between two or more groups is significantly greater than the difference within the intragroup to judge whether the grouping is reasonable. As shown in Fig.5A-B, Anosim analyse using weighted UniFrac distances and unweighted UniFrac respectively clustered samples and the results revealed that inter-mice variations of fecal microbiota were lower than intragroup which suggested that fecal microbiota of each group had better individual similarity. PCoA analysis showed that the distance between two samples are close which indicates that the species composition of the two samples is similar. As shown in Fig.5C-D, the results of PCoA analyses indicated the more similar the microbial composition between normal group and betaine group.

LDA EffectSize（LEfSe）analysis

LEfSe analysis emphasizes statistical significance and biological relevance. As shown in Fig.5E-F, a cluster tree displayed different colors represent different groups, and nodes of different colors represent corresponding important microorganisms in each group. However, the yellow node represented nonsignificant microbes. The 11 bacterial species in fecal samples, such as the *g-Bacteroide*, *f-Bacteroidaceae*, *o-Campylobacterales* and *c-Epsilonproteobacteria* which had a significant effect on normal group. *F-Lachnospiraceae*, *g-Enterorhabdus*, *o-Coriobacteriales* and *f-Coriobacteriaceae* controbuted to a great influence in model group. *G-Parabacteroides*, *g-Odoribacter*, *g-Prevotella*, *f-Oxalobacteraceae*, *g-Anaerovorax* and *f-Clostridiales-IncertaeSedisXIII* were of crucially importance in betaine group. As shown in Fig. 6A and Additional file 3, there were a total of 143 OTUs which had a significant difference between groups ($P < 0.05$). As shown in Fig. 6B-C and Additional file 4, there existed a total of 24 species which contained 11 species at the genus level which had a significant difference between groups ($P < 0.05$). At the genus level, they were *g-Anaeroplasma*, *g-Anaerovorax*, *g-Bacteroides*, *g-Desulfovibrio*, *g-Dorea*, *g-Enterorhabdus*, *g-Helicobacter*, *g-Odoribacter*, *g-Parabacteroides*, *g-Paraprevotella* and *g-Prevotella*. Among them, the increased relative abundance of *g-Enterorhabdus* in the model group was detected compared with normal group ($P < 0.05$). Betaine down-regulated the relative abundance of *g-Enterorhabdus* ($P < 0.05$). The relative abundance of *g-Bacteroides* was highest in normal group and least in model group ($P < 0.05$). The relative abundance of *g-Prevotella* is almost same in normal and betaine group, and was decreased in betaine group ($P < 0.05$).

Species classification and abundance analysis

A sequence with the highest abundance is selected from each OTU as a representative sequence of the OTU. Using the RDP method, the representative sequence is aligned with the 16S database to classify each OTU to corresponding species. Forming a relative abundance histogram of species, can visually observe the proportion of different species abundance in each sample and group. As shown in Fig. 7A-E and Fig. 8A-E, the corresponding histograms of species profiling were performed on each sample and group at the classification level of phylum, class, order, family, and genus. As shown in Fig. 8A and Additional file 5, the majority of the microbiome at the phylum levels among each group belonged to *Firmicutes*, *Bacteroidetes*, *Proteobacteria*, *Deferribacteres*, *Actinobacteria*, *Tenericutes*, *Verrucomicrobia* and *Candidatus Saccharibacteria*. Surprisingly, the majority of microbiome in phyla occupied similar proportions between normal group and ALF model group. Besides, *Firmicutes* was the most abundant phyla in each group. The relative abundance of *Firmicutes* in ALF model mice fecal (58.8%) was significantly higher than normal (42.5%) and betaine group (42.3%) ($P < 0.05$). And the relative abundance of *Bacteroidetes* in ALF model mice fecal (37.8%) was apparently lower than normal (50.2%) and betaine group (49.5%) ($P < 0.05$). As shown in Fig. 8E and additional file 6, the relative abundance of *Alistipes* (belonged to *Bacteroidetes*) was enriched in normal group (22.9%), and decreased in betaine

(18.8%) and model group (19.1%) (*P < 0.05*). The relative abundance of *Clostridium XlVa* (belonged to *Bacteroidetes*) was significant higher in ALF model group than normal group, and was reduced by betaine pretreatment in ALF model group (*P < 0.05*). There existed many differences of gut microbiome in mice fecal. These results indicated altering the gut microbiome might be crucial therapeutical target in ALF mice.

Discussion

Since 1998, when Marshall proposed the gut-liver axis, many attentions have been paid to the role of gut in liver disease [26]. Systemic endotoxemia, characterized by increased plasma LPS concentrations, increases the intestinal permeability such as altering tight junctions and thus lead to more endotoxins entering into the portal vein and activating the Kupffer cells in the liver. It results in producing pro-inflammatory cytokine and acute inflammatory response proteins which persistently aggravates hepatic insufficiency and/or failure [2]. Our previous study have indicated intestine injure plays a crucial role in the progress of ALF as well [27]. All these results support that if intestinal injury was reduced, and the liver lesion would be alleviated in ALF. Gut-liver axis pays an essential role in the pathogenesis in ALF.

Epithelial cells are held together by the apical junctional complex which including transmembrane proteins (such as claudins and occludin) and cytosolic scaffold proteins such as (ZO)-(1–3) and cingulin. The study has proved that inflammatory conditions contribute to significant disturbance of mucosal barrier function with a decreased expression and redistribution of claudin, (ZO)–1, and occludin which lead to increasing permeability [28]. LPS, which can trigger a powerful inflammatory response, is recognized as a causal or complicating factor of multiple serious diseases. One of the mechanisms which preventing LPS from intestine enter into the systemic circulation is through TLRs, which can activate the immune system [29]. However, the continuous stimulation of TLR signaling does not always provide positive effects for the host and it can enhance hepatic injury in NASH, alcoholic liver disease, and chronic viral hepatitis [30 - 32]. There are 11 TLRs which have been identified in mammals, whereas LPS binds mainly TLR4. The MyD88 dependent pathway, as one of the downstream signaling events mediated by TLR4, lead to the recruitment of numerous molecules, which results in the activation of transcription factors nuclear factor-B (NF-B), tumor necrosis factor (TNF-) and other proinflammatory factors [8]. It has proved that TNF- can down-regulate the expression of the transmembrane tight junction strand protein occludin, paralleling the barrier disturbance detected electrophysiologically which lead to an increase in intestinal permeability [33].

The intestinal epithelial barrier is not a static physical barrier but rather strongly interacts with the gut microbiome and cells of the immune system. Under physiological conditions, there is a dynamic regulation of tight junction components. However, sustained inflammation or infections can result in dysregulation in the expression of adhesion molecules, leading to barrier breach and disturbance of gut microbes [34]. The studies demonstrated that TLRs are innate pattern recognition receptors involved in host defense, normal over commensal bacteria and the maintenance of tissue integrity [35, 36]. The experiment has demonstrated that MyD88-negative mice with a defined microbial consortium which

representing bacterial phyla normally present in human gut [37]. It has been found that *B. adolescentis* exhibited anti-inflammatory properties in D-Gal treated rats. Accumulating evidence points to gut microbiota being involved in this process. The study has shown that *S. boulardii* significantly decreased in the relative abundance of phylum *Bacteroidetes,* and increased the relative abundance of *Firmicutes* and *Proteobacteria* in ALF mice [38].

Betaine, an oxidative metabolite of choline, can protect rats from induction of the LPS hepatotoxicity [39]. The present study showed that betaine exerts positive effects on gut-liver axis, including inhibition of potent inflammatory response and maintain the gut integrity. Our data showed that the TLR4 level was low in the healthy intestine and normal IEC18 cells. LPS induced an increased intestine TLR4 expression and aggregation. It was associated with an increase in MyD88, TRIF6 and TNF-α expression. In the meantime, there were low expression of (ZO)–1 and occludin in both animals and cells experiments after administrating with LPS. Notably, betatine ameliorates the small intestine damages and IEC–18 cell in model by reducing the high expression of TLR4, MyD88, TRAF6 and TNF-. Then the intestinal permeability in ALF mice and IEC–18 cell model was improved by enhancing the expression of the tight junction protein (ZO)–1 and occludin. Moreover, in cell experiments, the dose of betaine was positively correlated with its protective effect in model group.

And in our experiment, the 16s rRNA gene sequence analysis was used to explore the potential therapeutic microecological mechanisms of betaine on ALF mice. There were 156 core microbiomes in fecal samples. The fecal bacteria of normal group had the highest level of species richness and diversity. *F-Lachnospiraceae, g-Enterorhabdus, o-Coriobacteriales* and *f-Coriobacteriaceae* contributed to a great influence in ALF model group. The relative abundance of *g-Enterorhabdus* in the ALF model group was significant increased than normal group. *Enterorhabdus,* a member of the family *Coriobacteriaceae,* is isolated from a mouse model of spontaneous colitis [40]. The PCoA analysis showed that normal group and betaine group had more similar microbial composition. The relative abundance of *Firmicutes* in ALF model mice fecal was significantly higher than normal group. And the relative abundance of *Bacteroidetes* in ALF model mice fecal was apparently lower than normal group. But the bataine decreased the relative abundance of *Firmicutes* and increased the relative abundance of *Bacteroidetes* in ALF model. The previous study has been conformed the levels of *Firmicutes* were positive correlation with ACLF severity and *Bacteroidetes* were inversely correlated [8]. It exactly suggested that betaine played a role in potential modifying gut bacterial community. The taxon in gut microbitoa *Coriobacteriaceae, Lachnospiraceae, Enterorhabdus* and *Coriobacteriales* were remarkably increased in model group and contrary to the taxon in gut microbitoa *Bacteroidaceae, Bacteroides,Parabacteroides* and *Prevotella.* Betaine could significantly altered the microbial communities, depleting gut microbitoa *Coriobacteriaceae, Lachnospiraceae, Enterorhabdus* and *Coriobacteriales* and markedly enriching the taxa *Bacteroidaceae, Bacteroides,Parabacteroides and Prevotella.*

Conclusion

In summary, betaine improved liver function, liver and small intestine histology, intestine permeability and consolidated the tight connection between small intestine epithelial cells. The present study not only proved that betaine had hepatoprotective effect in ALF mice, but also further demonstrated its protection on structure and function of the small intestine. The one of the protective effect of betaine on small intestine in ALF is via inhibition of LPS/TLR4/MyD88 pathway and improving intestinal permeability and ultimately dramatically shaping the gut microbiota in mice. This work revealed a new role for betaine in improving hepatic lesion. These findings thus suggested that the compounds targeted on the gut-liver axis should be further investigated as novel adjunctive therapies for ALF. More clinical studies are supposed to verify the effective strategy to prevent and manage ALF by altering gut bacterial community.

Methods

Chemicals and reagents

Betaine hydrochlorides (99% of purity) were obtained by Juhua Group Co. (Zhejiang, China). Lipopolysaccharide (LPS, purity of 99%) and D-galactosamine (purity of 98%) were obtained from Sigma (St. Louis, USA). Fetal bovine serum (FBS) and DMEM basic were obtained from Gibco (NY, USA). Antibodies againgst TLR4 and (ZO)-1 were purchased from Proteintech (Hubei, China). Rabbit anti-rat/mice MyD88, TRAF6, TNF-α, occluding and β-actin were obtained from Cell Signaling Technology (Boston, USA). The Goat anti-rabbit fluorescent secondary antibody (IRDye800) was obtained from LI-COR Biosciences, Inc. (Lincoln, USA).

Cell culture

The rat small intestinal cell line IEC-18 was grown in DMEM medium mixed with 10 % FBS in an incubator at 37 °C, 5 % CO_2, and saturated humidity. LPS (1 μg/ml) were applied with cells in model group, low dose, medium dose and high dose betaine group. The cellular model was divided into normal group, model group, and betaine group. IEC-18 cells were seeded in 6-well plates. After 12 hours betaine (400 μg/ml, 600μg/ml and 800 μg/ml) was added respectively into low dose, medium dose and high dose betaine group, when model was conducted. After 24 h, the cells were detected by Western Blot and Quantitative real-time PCR.

Transepithelial electrical resistance (TEER) measurement

IEC-18 cell was made into 2.5×10^5 cells/ml single cell suspension. The lower cell chambers and the upper cell chambers were added with 1.5 ml DMEM complete medium and 1 ml cell suspension respectively. The upper and lower chambers in model and betaine group were replaced by the complete medium and complete medium contained betaine. After 2 h, betaine group and LPS group were added LPS at the same time. Normal group was added complete medium. Then all cells were incubated for 24 h. The calibrated Millipore Millicell ERS-2 cell resistance meter was used to detect resistance value. The measured resistance value was multiplied by the area of the filter to obtain an absolute value of TEER,

expressed as Ω•cm^2. And the TEER values were measured as follows: TEER = (measured resistance value - blank value) ´ single cell layer surface area (cm^2).

Animal groups

Eighteen male specific pathogen free (SPF) mice, weighing 20 ± 2g, were purchased from the Experimental Animal Center of Wuhan University. This study was approved by the Ethics Committee of Renmin Hospital of Wuhan University. All animals were allowed access to food and water freely throughout the acclimatization and experimental periods. And they were kept in temperature (22 ± 2 °C) with a 12 h light/dark cycle. After acclimation for 1 week, animals were randomly divided into three groups: normal, model, betaine group. The ALF model was induced by D-Gal (400 mg/kg) and LPS (100 μg/ml) by intraperitoneal injection. Betaine groups were administrated intragastrically with betaine 800 mg/kg per day one week before ALF model was conducted. The other mice were administrated intragastrically with same amount of saline. All mice were sacrificed in 24 h after the mice of model and betaine groups were given D-Gal/LPS.

Assessment of liver function and serum inflammatory mediators

Blood samples were collected. The serum alanine aminotransferase (ALT), aspartate aminotransferase (AST) and total bilirubin (TBil) levels were assayed using routine biochemical methods by a Hitachi Automatic Analyzer (Hitachi, Inc, Japan). The serum inflammatory cytokine levels of tumour necrosis factor α (TNF-α), interleukin-1β (IL-1β) and IL-18 were detected by enzyme-linked immunosorbent assay (ELISA) kits (eBioscience, CA, USA)

Histological examinations

Liver and small intestine specimens were fixed in 10 % formaldehyde for 24 h, embedded in paraffin, sliced into sections of 5 μm thickness and stained with hematoxylin-eosin (HE). Histological assessment was evaluated under BX 51 light microscope (Olympus, Japan).

Western blotting

The IEC-18 cells and small intestine specimens extracts were subjected to 10 % sodium dodecyl sulfate–polyacrylamidem gelelectrophoresis (SDS-PAGE) and transferred to a protran nitrocellulose membrane (Millipore, Merck KGaA, Darmstadt, Germany). The membrane was sequential incubated with primary antibody at 4 °Covernight and secondary antibody at 1 h (LI-COR Co, Lincoln), detected by Odyssey infrared imaging system (LI-COR Co). The protein levels of TLR4, MyD88, TRAF6, TNF-a, (ZO)-1, occludin were normalized to β-actin for each sample. The dilutions of the primary and secondary antibodies were as follows: TLR4, 1:1000; MyD88, 1:1000; TRAF6, 1:1,000; TNF-a,1:1,000; (ZO)-1, 1:1,000; occludin, 1:10,000; and β-actin,1:1,000 respectively.

Quantitative real-time PCR

Total RNA was extracted from IEC-18 cells and the small intestine specimens by use of TRIzol reagent according to the manufacturer's procedure. The cDNAs were produced with a PrimeScript RT reagent kit by use of the following methods: 2 mg RNA, 0.5 mg oligo $(dT)_{15}$ primer, and DEPC (diethyl-pyrocarbonate)-treated water were added to a total volume of 15 mL mixture at 85 ℃ for 5 min, then rapidly chilled on ice. Quantitative real-time polymerase chain reaction was performed with complementary DNA using the SYBR Premix Ex Taq kit by use of a StepOne Plus device (Applied Biosystems) at 95 °C for 10 s, followed by 40 cycles of 95 °C for 5 s and 60 °C for 20 s. All the primer sequence (Table 1) were designed and synthesized by Tsingke (Wuhan, China). β-actin was set as the housekeeping gene.

Intestinal permeability

The everted sac method was used as previously described to evaluate the small intestinal mucosal barrier function [27]. First, we everted the intestine segment in ice-cold Krebs buffer (pH 7.4), gently distended by injecting 1.5 mL of Krebs, and then suspended in the organ bath which contained 500 mL Krebs with added FITC-labeled dextran 4000 (FD4, 10 mg/mL) and maintained at 37 ˚C, continuously bubbled with a gas mixture containing 95 % O_2 and 5 % CO2 for 30 min. Finally, Samples from the sac were centrifuged at 1000 g, 4 ˚C for 5 min. FD 4 concentration was detected at an excitation wavelength of 492 nm and an emission wavelength of 515 nm with Perkin-Elmer LS-50 fluorescence spectrophotometer (PerkinElmer Inc, Waltham, MA). Intestinal permeability was expressed as FD4 concentration divided by the area of gut sac.

DNA extraction and 16s rRNA gene sequencing

Fecal samples of mouse were collected 1 hour before all animals sacrificing. And they were frozen at -80 °C. DNA was extracted using the QIAGEN extraction kit (Universal Biotech Company, Shanghai, China) and total DNA quality was assessed using the Thermo Qubit.

Sequencing library construction

The V3-4 region of the 16s rRNA gene was amplified using custom barcoded primers and sequenced as described previously using an Illumina MiSeq sequencer [41, 42]. Briefly, the V3-4 domain of the 16S rRNA gene was amplified using primers F (5'-NNNNNNNNGTGTGCCAGCMGCCGCGGTAA-3') and R (5'-GGACTACHVGGGTWTCTAAT-3'). Using diluted genomic DNA as a template, PCR was performed using Taq DNA Polymerase (Vazyme Biotech Company, Nanjing, China) to ensure the accuracy and efficiency of amplification. The PCR product library was examined by Fragment Analyzer. After the library quality inspection was eligible, the corresponding ratios were mixed according to the volume required in each sample. The mixed library was subjected to gelatinization purification (cutting range: 500-750 bp) using a

QIAquick gel recovery kit (Universal Biotech Company, Shanghai, China). After recycling, the library was examined and quantified using a Fragment Analyzer and an Applied Biosystems QuantStudio 6 real-time PCR instrument. Sequencing was performed using Illumina MiSeq PE300.

After performing quality control of the original data, the Usearch software was used to de-chimerize and cluster the data. When Usearch clusters, Reads were first sorted according to the abundance from large to small, and the standard clustering of 97 % similarity is obtained. Each Operational Taxonomic Units (OTU) was considered to represent a species. Next, the Reads of each sample were randomly leveled and the corresponding OTU sequence was extracted. Then we used Qiime software to do the dilution curve of Alpha diversity index, selected reasonable sampling parameters according to the dilution curve, and analyzed the obtained OTU. A read was extracted as a representative sequence from OTU. Next, the representative sequence was aligned with the 16S database to classify each OTU by using the RDP method. After categorization, the OTU abundance table was obtained according to the number of sequences in each OTU. Finally, the subsequent analysis was performed according to the OTU abundance table [43].

Statistical analysis

The all results were presented as mean ± SE. Comparisons of the measurement data among groups were assessed with Student's t test and one-way analysis of variance (ANOVA). P value < 0.05 was considered statistically significant. Calculations were performed with the SPSS16.0 statistical software package. Alpha diversity was applied in analyzing complexity of species diversity for single sample through 4 indices including observed species, chao1, shannon and simpon. Beta diversity analysis was used to evaluate differences of samples in species complexity. LEfSe was used by linear discriminant analysis (LDA) to estimate the influence of each species abundance to identify communities or species that have significant differences in sample partitioning.

Additional File

Additional file 1: OTU network analyses showed 509 specific OTUs were produced from 15 fecal samples. (TSV 38kb)

Addition file 2: OTU network analyses showed 156 core microbiome in all fecal samples. (TSV 5kb)

Addition file 3: LEfSe analysis showed 143 specific OTUs which had a significant difference between groups. (TXT 7kb)

Addition file 4: LEfSe analysis showed 24 specific species which had a significant difference between groups. (TXT 6kb)

Additional file 5: Each phylum microbiome occupied the specific proportion of in each group feces. (TXT 2kb)

Addition file 6: Each genus microbiome occupied the specific proportion of in each group feces. (TXT 5kb)

Abbreviations

ALF: acute liver failure; LPS: Lipopolysaccharide; D-Gal: D-galactosamine; ALT: alanine aminotransferase; AST: aspartic transaminase; TBIL: total bilirubin; (ZO)–1: Zonula occludens–1; TLR4: Toll-like receptor 4; MyD88: myeloid differentiation factor 88; TRAF6: Tumor necrosis factor receptor-associated factor 6; TNF-α: tumor necrosis factor α; IL–1β: interleukin–1β; IL–18: interleukin–18; OTU: operational taxonomic unit; LDA: linear discriminant analysis; PCoA: Principal Coordinates Analysis.

Declarations

Acknowledgements

The authors would like to thank the central laboratory at Renmin Hospital of Wuhan University (Wuhan, Hubei, China) for their technical supports.

Authors' contributions

ZJG designed the study and revised the manuscript. QC and YW carried out experiments and performed the bioinformatic and statistical analysis. QC and LWW wrote the manuscript. FZJ, MHP and CXS helped to perform experiments. All authors read and approved the final manuscript.

Availability of data and materials

The OTU network analyses data was available as Additional file 1 and Additonal file 2.

LEfSe analysis data were submitted as Addition file 3 and Addition file 4.

Ethics approval

All animal experiments were performed in accordance with the institutional guidelines of the Animal Care and Use Committee of Renmin Hospital of Wuhan University and the Guide for the Care of Laboratory Animals published by the US National Institutes of Health (NIH publication no. 85-23, revised 1996).

Consent for publication

Not applicable

Competing interests

The authors declare that they have no competing interests.

Author details

[1]Department of Infectious Diseases, Renmin Hospital of Wuhan University, Wuhan 430060, China

References

[1] William M. L. Recent Developments in Acute Liver Failure. Best Pract Res Clin Gastroenterol. 2021;26(1):3-16.

[2] Han DW. Intestinal endotoxemia as a pathogenetic mechanism in liver failure. World J Gastroenterol. 2002;8:961e965.

[3] Jalan R, Williams R. Acute-on-chronic liver failure: pathophysiological basis of therapeutic options. Blood Purif. 2002;20:252e261.

[4] Patterson AM, Watson AJM. Deciphering the Complex Signaling Systems That Regulate Intestinal Epithelial Cell Death Processes and Shedding. Front Immunol. 2017;8:841.

[5] Han X, Fink MP, Yang R, Delude RL. Increased iNOS activity is essential for intestinal epithelial tight junction dysfunction in endotoxemic mice. Shock. 2004;21(3):261-70.

[6] Scaldaferri F, Pizzoferrato M, Gerardi V, Lopetuso L, Gasbarrini A.The Gut Barrier New Acquisitions and Therapeutic Approaches. J Clin Gastroenterol. 2012;Suppl:S12-7.

[7] Istvan ES□Deisenhofer J□ Structural mechanism for statin inhibition of HMG CoA reductase□ Science□ 2001;292(5519):1160□

[8] Kawai T, Akira S. The role of pattern-recognition receptors in innate immunity: update on Toll-like receptors. Nat Immunol. 2010;11(5):373-84.

[9] Doyle SL, O'Neill LA. Toll-like receptors: from the discovery of NFkappaB to new insights into transcriptional regulations in innate immunity. Biochem Pharmacol. 2006;72(9):1102-13.

[10] Arancibia SA, Beltrán CJ, Aguirre IM, Silva P, Peralta AL, Malinarich F, et al. Toll-like receptors are key participants in innate immune responses. Biol Res. 2007;40(2):97-112.

[11] Wang H, Li Y. Protective effect of bicyclol on acute hepatic failure induced by lipopolysaccharide and D-galactosamine in mice. Eur J Pharmacol. 2006;534(1-3):194-201.

[12] Tranah TH, Vijay GK, Ryan JM, Shawcross DL. Systemic inflammation and ammonia in hepatic encephalopathy. Metab Brain Dis. 2013;28(1):1-5.

[13] Jiang W, Wu N, Wang X, Chi Y, Zhang Y, Qiu X, et al. Dysbiosis gut microbiota associated with inflammation and impaired mucosal immune function in intestine of humans with non-alcoholic fatty liver disease. Sci Rep. 2015;5:8096.

[14] Sarin SK, Choudhury A. Acute-on-chronic Liver Failure. Curr Gastroenterol Rep.2016;18(12):61.

[15] Verbeke L, Nevens F, Laleman W. Bench-to-beside review: acute-on-chronic liver failure - linking the gut, liver and systemic circulation. Crit Care. 2011;15(5):233. doi: 10.1186/cc10424.

[16] Li Y, Lv L, Ye J, Fang D, Shi D, Wu W, et al. Bifidobacterium adolescentis CGMCC 15058 alleviates liver injury, enhances the intestinal barrier and modifies the gut microbiota in D-galactosamine-treated rats. Appl Microbiol Biotechnol. 2019;103(1):375-393.

[17] Chen Y, Guo J, Qian G, Fang D, Shi D, Guo L, et al. Gut dysbiosis in acute-on-chronic liver failure and its predictive value for mortality. J Gastroenterol Hepatol. 2015;30(9):1429-37.

[18] Bischoff SC, Barbara G, Buurman W, Ockhuizen T, Schulzke JD, Serino M, et al. Intestinal permeability–a new target for disease prevention and therapy. BMC Gastroenterol. 2014;14:189.

[19] Day CR, Kempson SA. Betaine chemistry, roles, and potential use in liver disease. Biochim Biophys Acta. 2016;1860 (6):1098-106.

[20] Ganesan B, Anandan R. Protective effect of betaine on changes in the levels of lysosomal enzyme activities in heart tissue in isoprenaline-induced myocardialinfarction in Wistar rats. Cell Stress Chaperones. 2009;14 (6):661-7.

[21] Bingül İ, Başaran-Küçükgergin C, Aydın AF, Çoban J, Doğan-Ekici I, Doğru-Abbasoğlu, et al. Betaine treatment decreased oxidative stress, inflammation, and stellate cell activation in rats with alcoholic liver fibrosis. Environ Toxicol Pharmacol. 2016;45:170-178.

[22] Zhou RF, Chen XL, Zhou ZG, Zhang YJ, Lan, QY, Liao GC, et al. Higher dietary intakes of choline and betaine are associated with a lower risk of primary liver cancer: a case-normal study. Sci Rep. 2017;7 (1):679.

[23] Chen YM, Liu Y, Zhou RF, Chen XL, Wang C, Tan XY, et al. Associations of gut-flora-dependent metabolite trimethylamine-N-oxide, betaine and choline with non-alcoholic fatty liver disease in adults. Sci Rep. 2016;6:19076.

[24] Shi QZ, Wang LW, Zhang W, Gong ZJ. Betaine inhibits toll-like receptor 4 expression in rats with ethanol-induced liver injury. World J Gastroenterol. 2010;16 (7):897-903.

[25] Zhang W, Wang LW, Wang LK, Li X, Zhang H, Luo LP, et al. Betaine protects against high-fat-diet-induced liver injury by inhibition of high-mobility group box 1 and Toll-like receptor 4 expression in rats. Dig Dis Sci.2013;58 (11):3198-206.

[26] Marshall JC. The gut as a potential trigger of exercise-induced inflammatory responses. Can J Physiol Pharmacol. 1998;76(5):479-84.

[27] Zhang Q, Yang F, Li X, Zhang HY, Chu XG, Zhang H, et al. Trichostatin A protects against intestinal injury in rats with acute liver failure. J Surg Res. 2016;205(1):1-10.

[28] Sánchez de, Medina F, Romero-Calvo I, Mascaraque C, Martínez-Augustin O. Intestinal inflammation and mucosal barrier function. Inflamm Bowel Dis. 2014;20(12):2394-404.

[29] Guerville M, Boudry G. Gastrointestinal and hepatic mechanisms limiting entry and dissemination of lipopolysaccharide into the systemic circulation. Am J Physiol Gastrointest Liver Physiol. 2016;311 (1):G1-G15.

[30] Miura K, Kodama Y, Inokuchi S, Schnabl B, Aoyama T, Ohnishi H, et al. Toll-like receptor 9 promotes steatohepatitis by induction of interleukin-1beta in mice. Gastroenterology. 2010;139:323-324.

[31] Inokuchi S, Tsukamoto H, Park E, Liu ZX, Brenner DA, Seki E. Toll-like receptor 4 mediates alcohol-induced steatohepatitis through bone marrow-derived and endogenous liver cells in mice. Alcohol Clin Exp Res. 2011;35:1509-1518.

[32] Dhillon N, Walsh L, Krüger B, Ward SC, Godbold JH, Radwan M, et al. A single nucleotide polymorphism of Toll-like receptor 4 identifies the risk of developing graft failure after liver transplantation. J Hepatol. 2010;53:67-72.

[33] Mankertz J, Tavalali S, Schmitz H, Mankertz A, Riecken EO, Fromm M, et al. Expression from the human occludin promoter is affected by tumor necrosis factor alpha and interferon gamma. J Cell Sci. 2000;113:2085-90.

[34] Takiishi T, Fenero CIM, Câmara NOS. Intestinal barrier and gut microbiota: Shaping our immune responses throughout life. Tissue Barriers. 2017;5(4):e1373208.

[35] Rakoff-Nahoum S, Paglino J, Eslami-Varzaneh F, Edberg S, Medzhitov R. Recognition of commensal microflora by toll-like receptors is required for intestinal homeostasis. Cell. 2004;118:229–41.

[36] Caputi V, Marsilio I, Cerantola S, Roozfarakh M, Lante I, Galuppini F, et al. Toll-Like Receptor 4 Modulates Small Intestine Neuromuscular Function through Nitrergic and Purinergic Pathways. Front Pharmacol. 2017;8:350.

[37] Wen L, Ley RE, Volchkov PY, Stranges PB, Avanesyan L, Stonebraker AC, et al. Innate immunity and intestinal microbiota in the development of Type 1 diabetes. Nature. 2008;455(7216):1109-13.

[38] Yu L, Zhao XK, Cheng ML, Yang GZ, Wang B, Liu HJ, et al. Saccharomyces boulardii Administration Changes Gut Microbiota and Attenuates D-Galactosamine-Induced Liver Injury. Sci Rep. 2017;7(1):1359.

[39] Kim SK, Kim YC. Attenuation of bacterial lipopolysaccharide-induced hepatotoxicity by betaine or taurine in rats. Food Chem Toxicol. 2002;40(4): 545-9.

[40] Clavel T, Duck W, Charrier C, Wenning M, Elson C, Haller D. Enterorhabdus caecimuris sp. nov., a member of the family Coriobacteriaceae isolated from a mouse model of spontaneous colitis, and emended description of the genus Enterorhabdus Clavel et al. 2009. Int J Syst Evol Microbiol. 2010;60:1527-31.

[41] Kozich JJ, Westcott SL, Baxter NT, Highlander SK, Schloss PD. Development of a dual-index sequencing strategy and curation pipeline for analyzing amplicon sequence data on the MiSeq Illumina sequencing platform. Appl Environ Microbiol. 2013;79(17):5112-20.

[42] Schloss P: Data File Repository for the Manuscript, Structure of the Gut Microbiome Following Colonization with Human Feces Determines Colonic Tumor Burden by Niel Baxter, Joseph Zackular and Colleagues.

[43] Langille MG, Zaneveld J, Caporaso JG, McDonald D, Knights D, Reyes JA, et al. Predictive functional profiling of microbial communities using 16S rRNA marker gene sequences. Nat Biotechnol. 2013;31(9):814-21.

Table

Table1: The primer sequence for RT-PCR.

Genes	Forward (5′-3′)	Reverse (5′-3′)
TLR4(rat)	TACAGTTCGTCATGCTTTCTC	ATTAGGAAGTACCTCTATGCAG
TLR4(mouse)	AGCTTCTCCAATTTTTCAGAACTTC	TGAGAGGTGGTGTAAGCCATGC
MyD88(rat)	AGGACAAACGAAGGAACTTTT	GCCGATAGTCTGTCTGTTCTAGT
MyD88(mouse)	ACCTGTGTCTGGTCCATTGCCA	GCTGAGTGCAAACTTGGTCTGG
(ZO)-1(rat)	GCTCACCAGGGTCAAAATGT	GGCTTAAAGCTGGCAGTGTC
(ZO)-1(mouse)	GTTGGTACGGTGCCCTGAAAGA	GCTGACAGGTAGGACAGACGAT
Occludin(rat)	TTACGGCTATGGAGGGTACAC	GACGCTGGTAACAAAGATCAC
Occludin(mouse)	TGGCAAGCGATCATACCCAGAG	CTGCCTGAAGTCATCCACACTC
β-actin(rat)	GTCGTACCACTGGCATTGTG	CTCTCAGCTGTGTGTGTGAA
β-actin(mouse)	CTCTCAGCTGTGTGTGTGAA	TGCTGGAAGGTGGACAGTGAGG

Figures

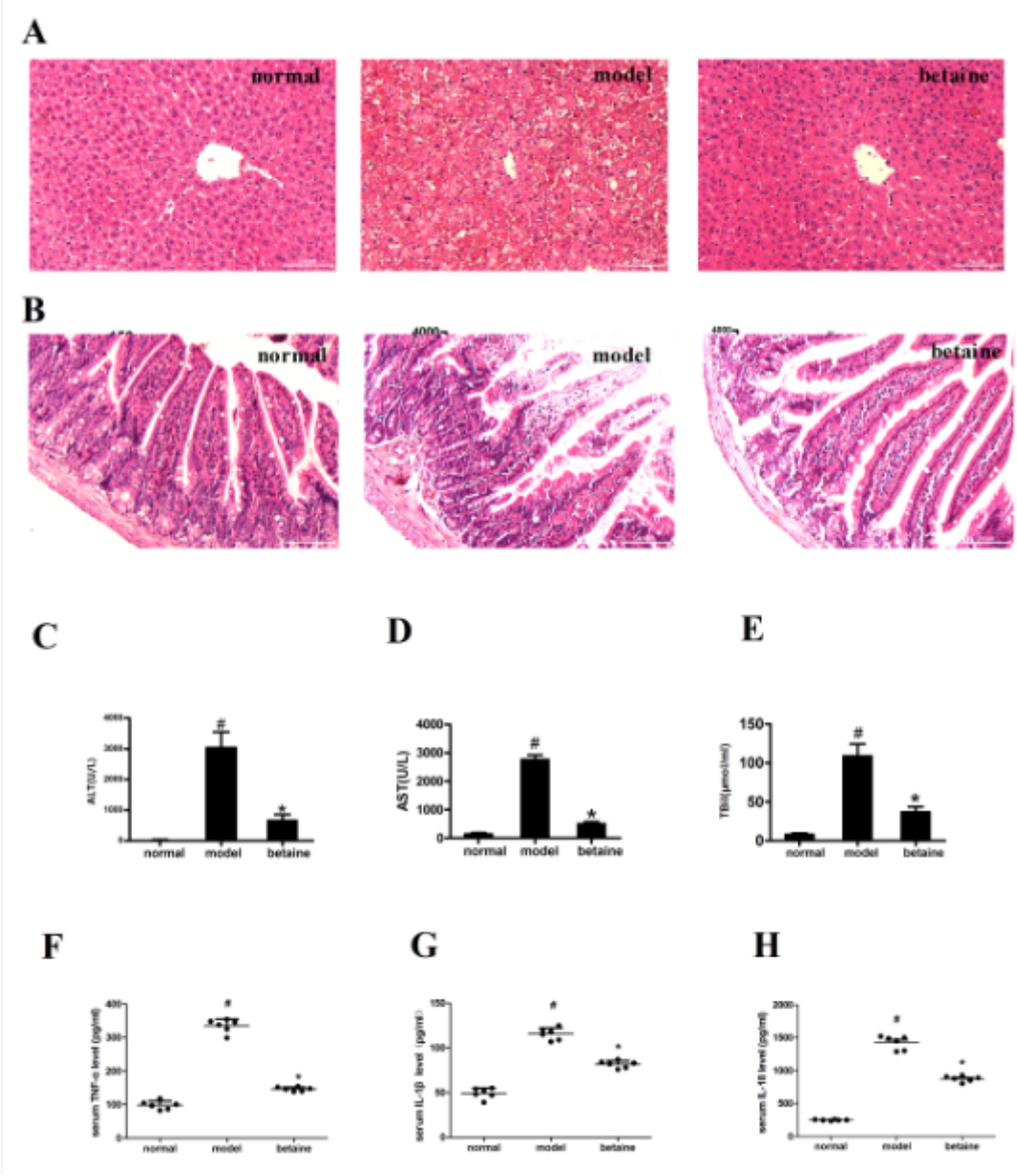

Figure 1

Effect of ACY1216 on live and small intestine tissue pathological changes and serum biochemical indicators in ALF mice. (A) The liver tissues were stained with HE (200 ×). (B) The small intestine tissue tissues were stained with HE (200 ×). (C-E) The serum levels of ALT, AST, and TBIL in different animal group. # P < 0 05, compared with normal group; * P < 0.05, compared with model group. (F-H) The serum levels of TNF-α, IL-1β and IL-18 in each group. Compared with normal group, # P < 0.05; Compared with ALF group, * P < 0.05.

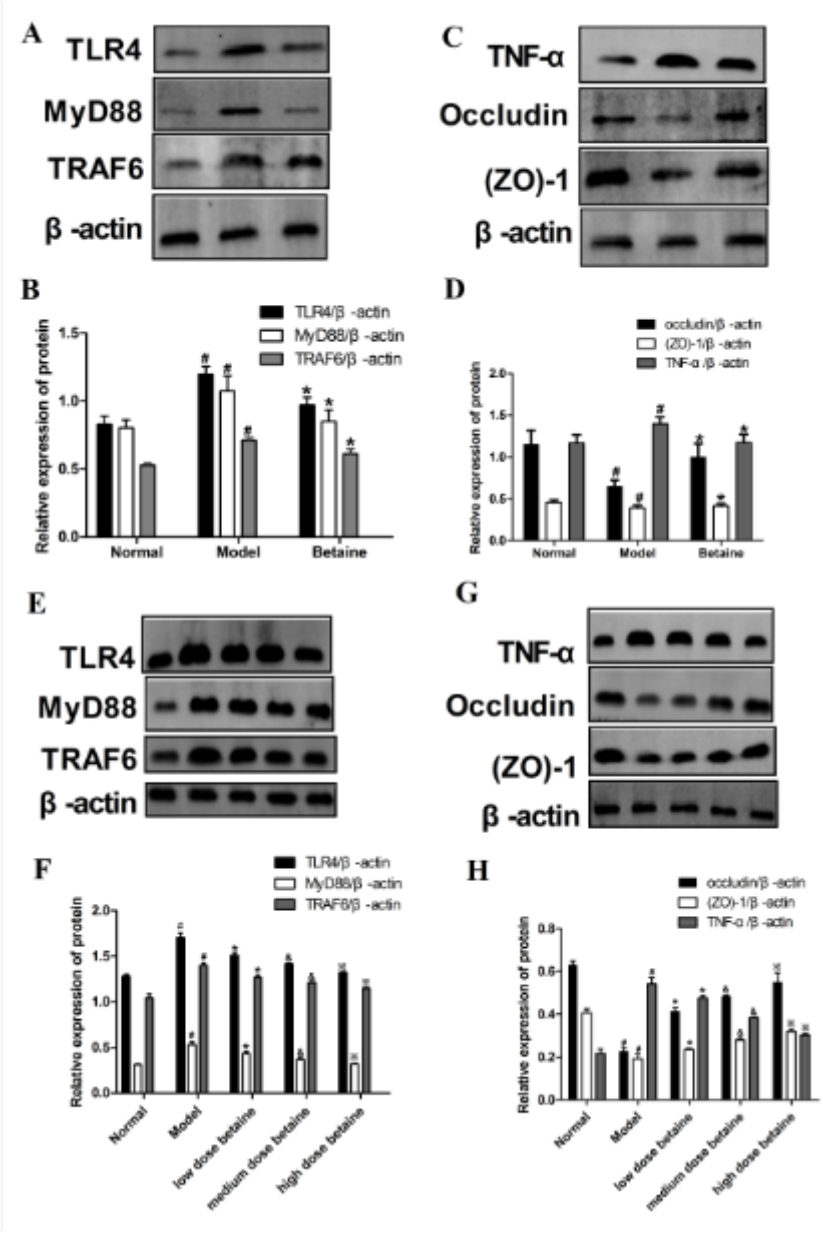

Figure 2

Effect of ACY1215 on the TLR4/MyD88 pathway, (ZO)-1 and occludin protein levels in ALF mice and LPS-stimulated IEC-18 cell. (A-D) The small intestine tissue protein levels of TLR4, MyD88, TRAF6, TNF-α, (ZO)-1 and occludin in each animal group. (E-H) The protein levels of TLR4, MyD88, TRAF6, TNF-α, (ZO)-1 and occludin in each IEC-18 cell group. # P < 0 05, compared with normal group; * P < 0 05, compared with model group; & P < 0 05, compared with the low dose betaine group; ※ P < 0 05, compared with the medium dose betaine group.

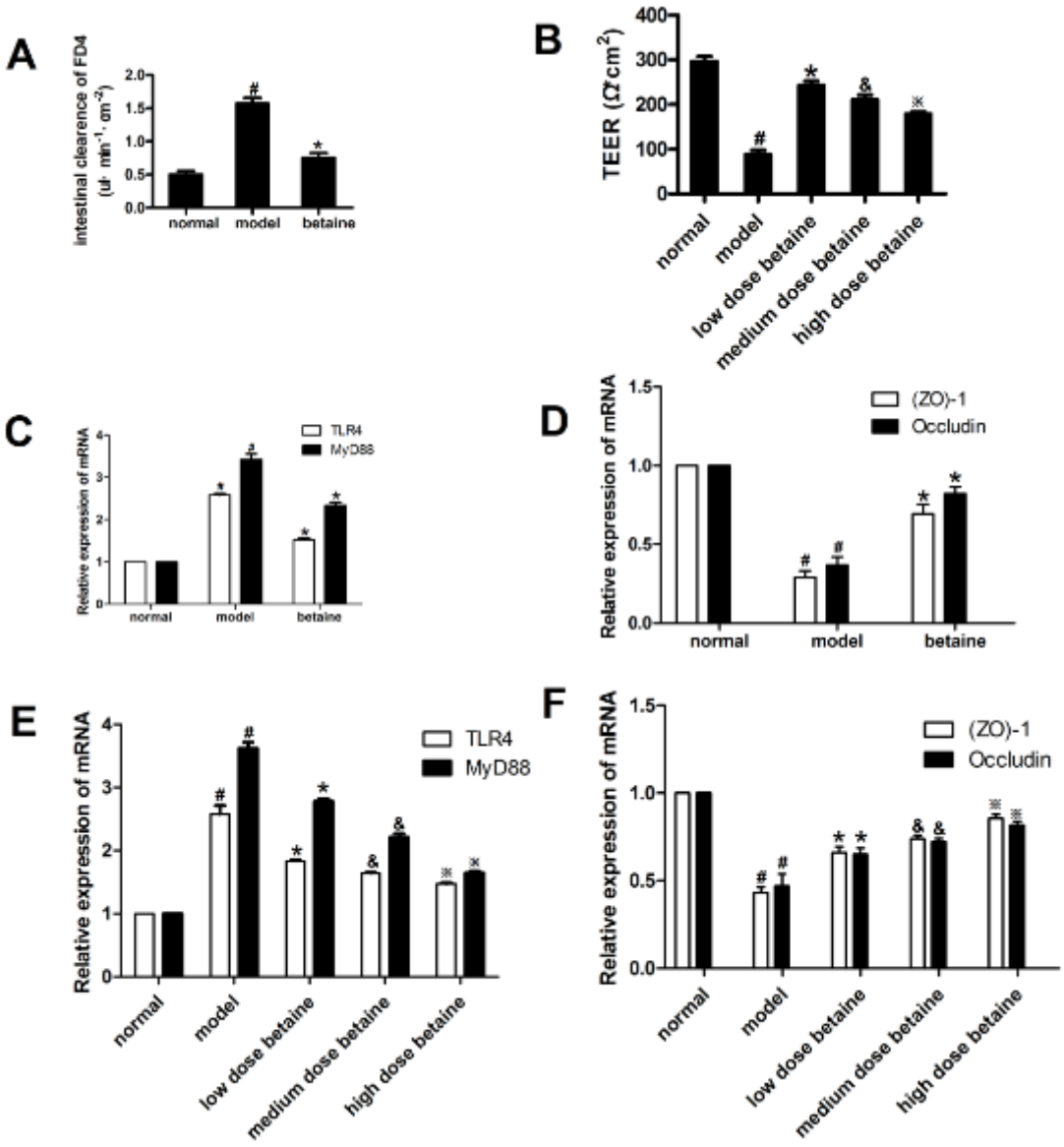

Figure 3

Effect of ACY1215 on the TLR4/MyD88 pathway, (ZO)-1 and occludin mRNA levels and intestinal permeability in ALF mice and LPS-stimulated IEC-18 cell. (A) The intestinal permeability in each animal group. (B) The TEER value in different cell group. (C-D) The mRNA levels of TLR4, MyD88, (ZO)-1 and occludin in different animal group. (E-F) The mRNA levels of TLR4, MyD88, (ZO)-1 and occludin in different cell group. # P < 0 05, compared with normal group;* P < 0.05, compared with model group; & P < 0 05, compared with the low dose betaine group; ※ P < 0 05, compared with the medium dose betaine group.

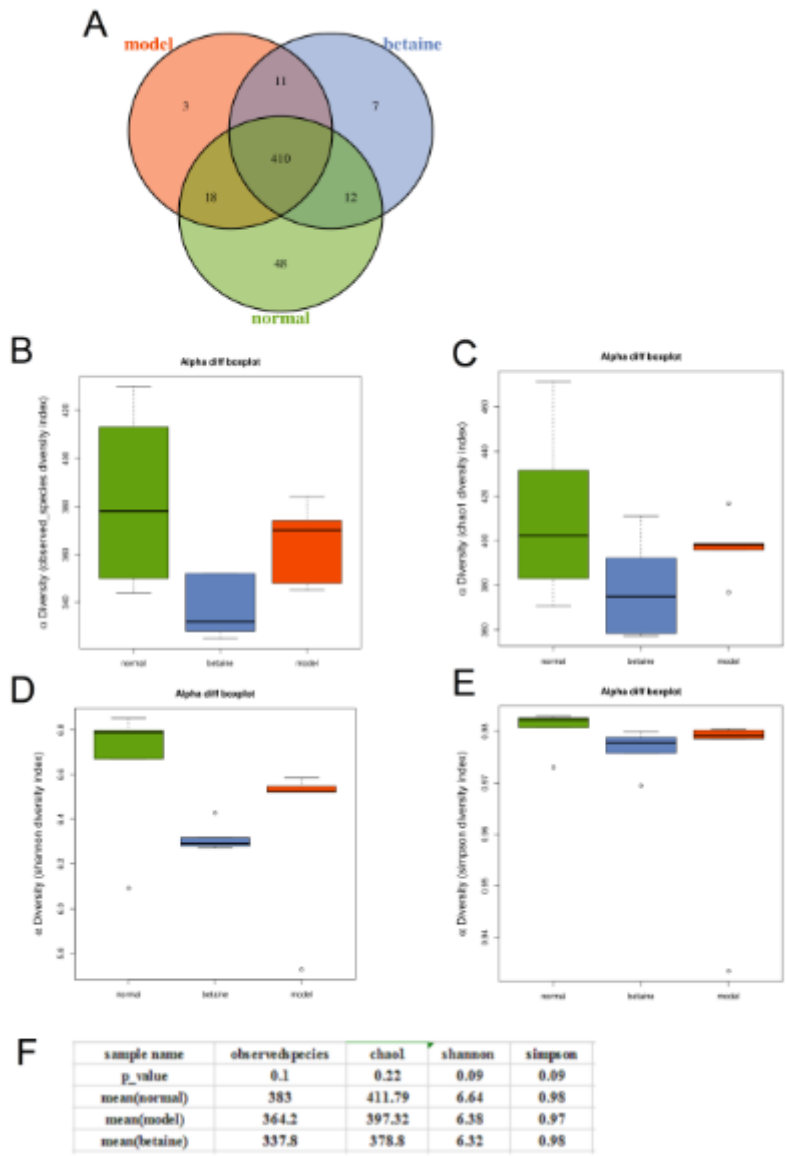

F

sample name	observed species	chao1	shannon	simpson
p_value	0.1	0.22	0.09	0.09
mean(normal)	383	411.79	6.64	0.98
mean(model)	364.2	397.32	6.38	0.97
mean(betaine)	337.8	378.8	6.32	0.98

Figure 4

OTU analysis and Alpha diversity analysis. (A) OTU venn diagram showed different color patterns represented different groups, and the number of overlaps between different color patterns was the number of OTUs shared between two groups. (B-E) Alpha diversity analysis:observed species (B), Chao 1 (C), Shannon (D) and Simpson (E) indexes of each samples. (F) Alpha diversity analysis table: The first row was the Alpha diversity name; the second row was the p-value of the rank sum test corresponding to the Alpha diversity index; the third row to the fifth row were the average mean of the three group samples.

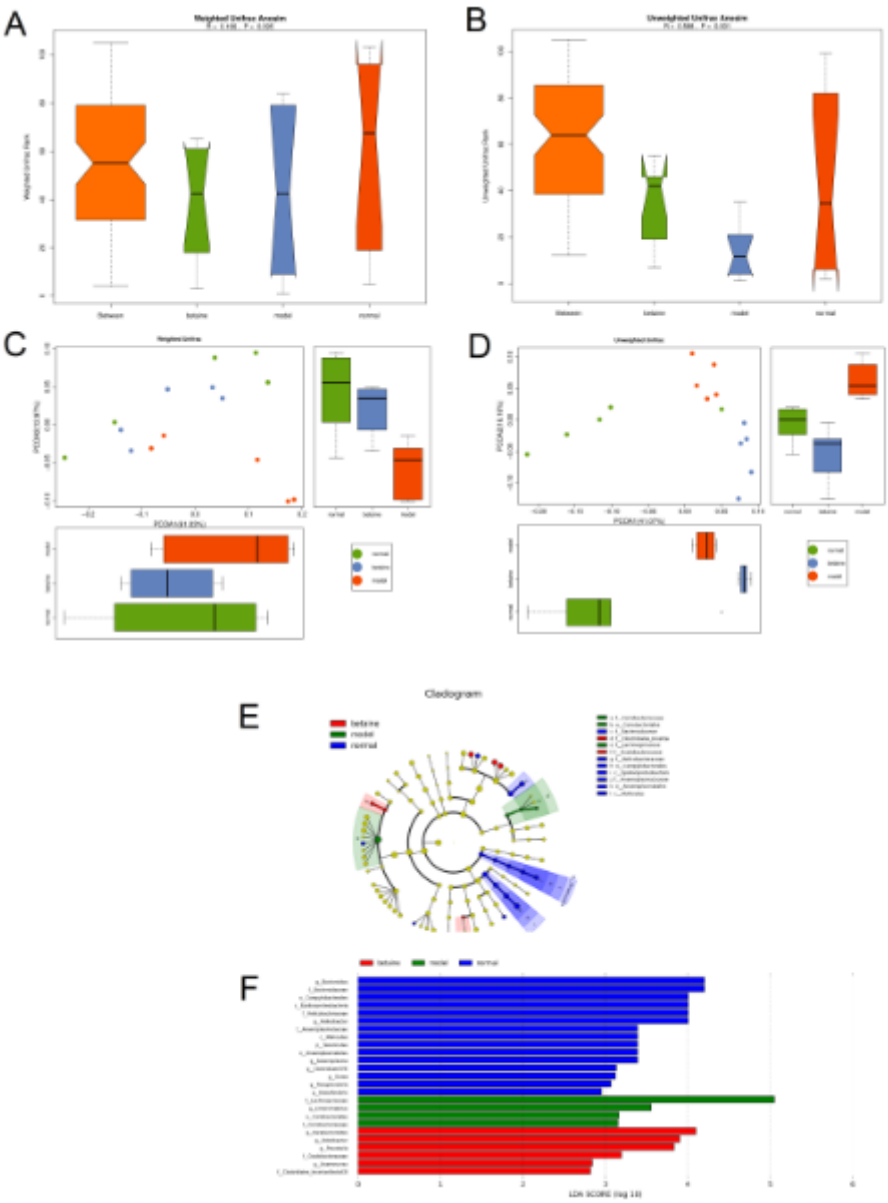

Figure 5

Beta diversity contained the Anosim analyse and PCoA analyses. (A-B) weighted UniFrac Anosim analyse and unweighted UniFrac Anosim;(C-D) weighted UniFrac PCoA analyses and unweighted PCoA analyses. (E-F) LEfSe analyses showed a cluster tree (E) and histogram (F) represented the gut bacteria which is of important biological significance in each group.

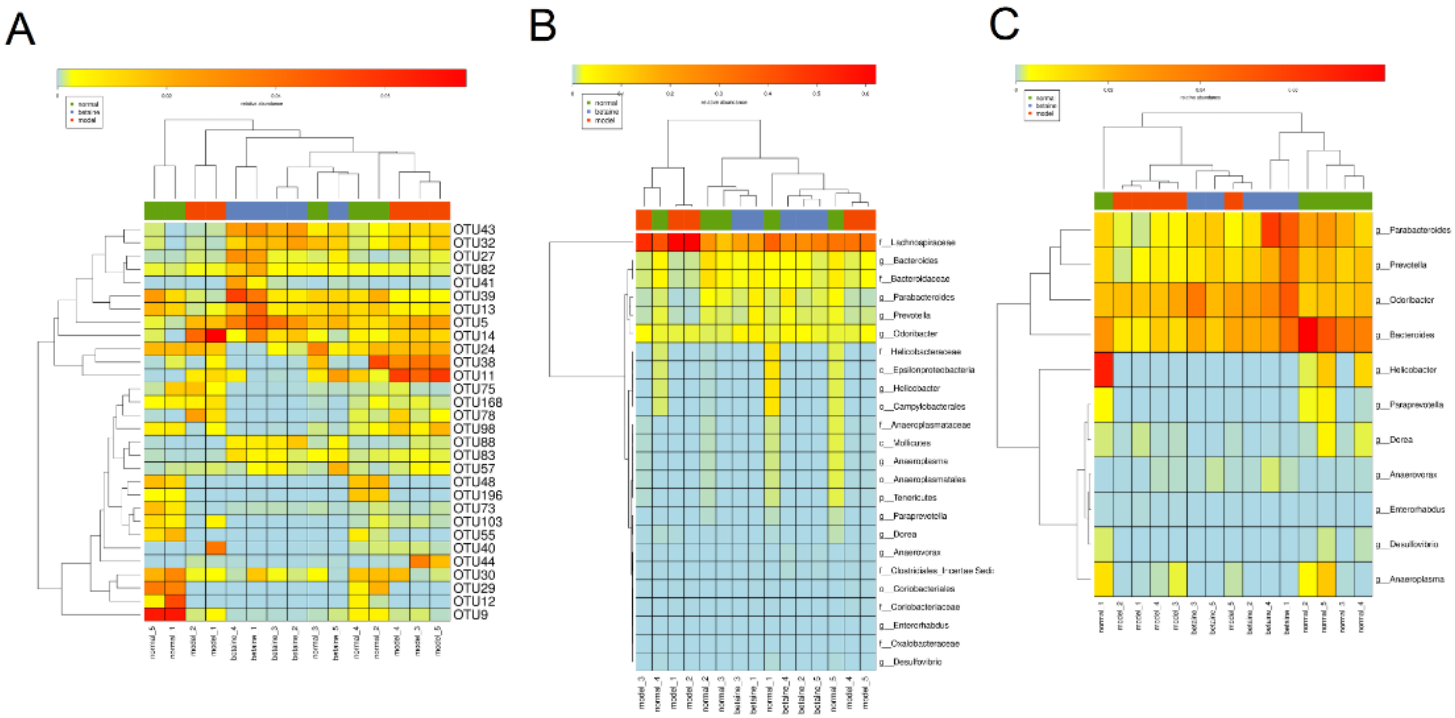

Figure 6

LEfSe analyses showed three Heatmaps. (A) The OTUs which have a significant differences between different groups. (B) A total of 24 species which have significant differences between groups. (C) There 11 genus species which have a significant differences between groups.

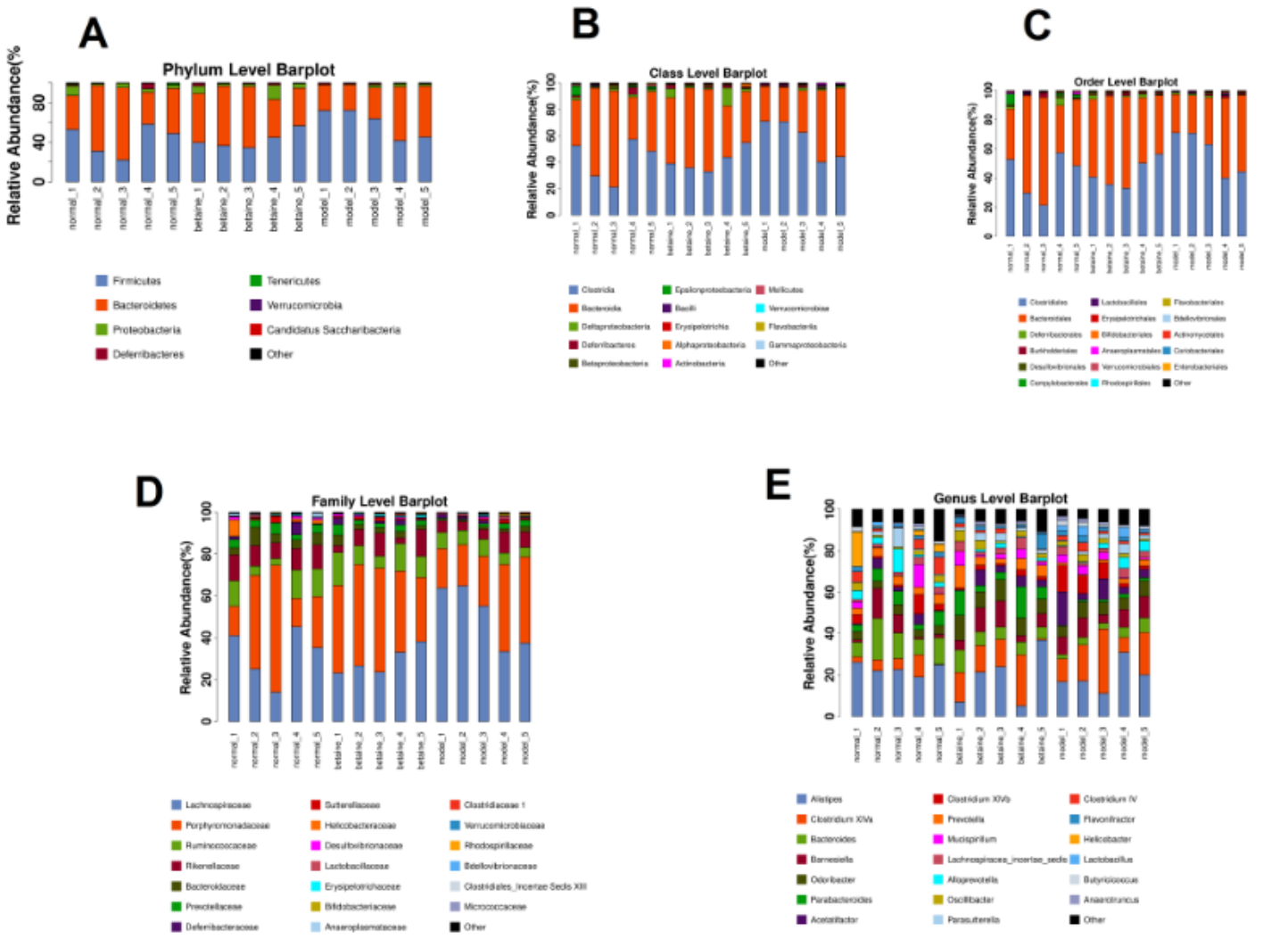

Figure 7

Species classification and abundance analysis. (A-E) The corresponding histograms of species profiling were performed on each sample at the classification level of phylum, class, order, family, and genus.

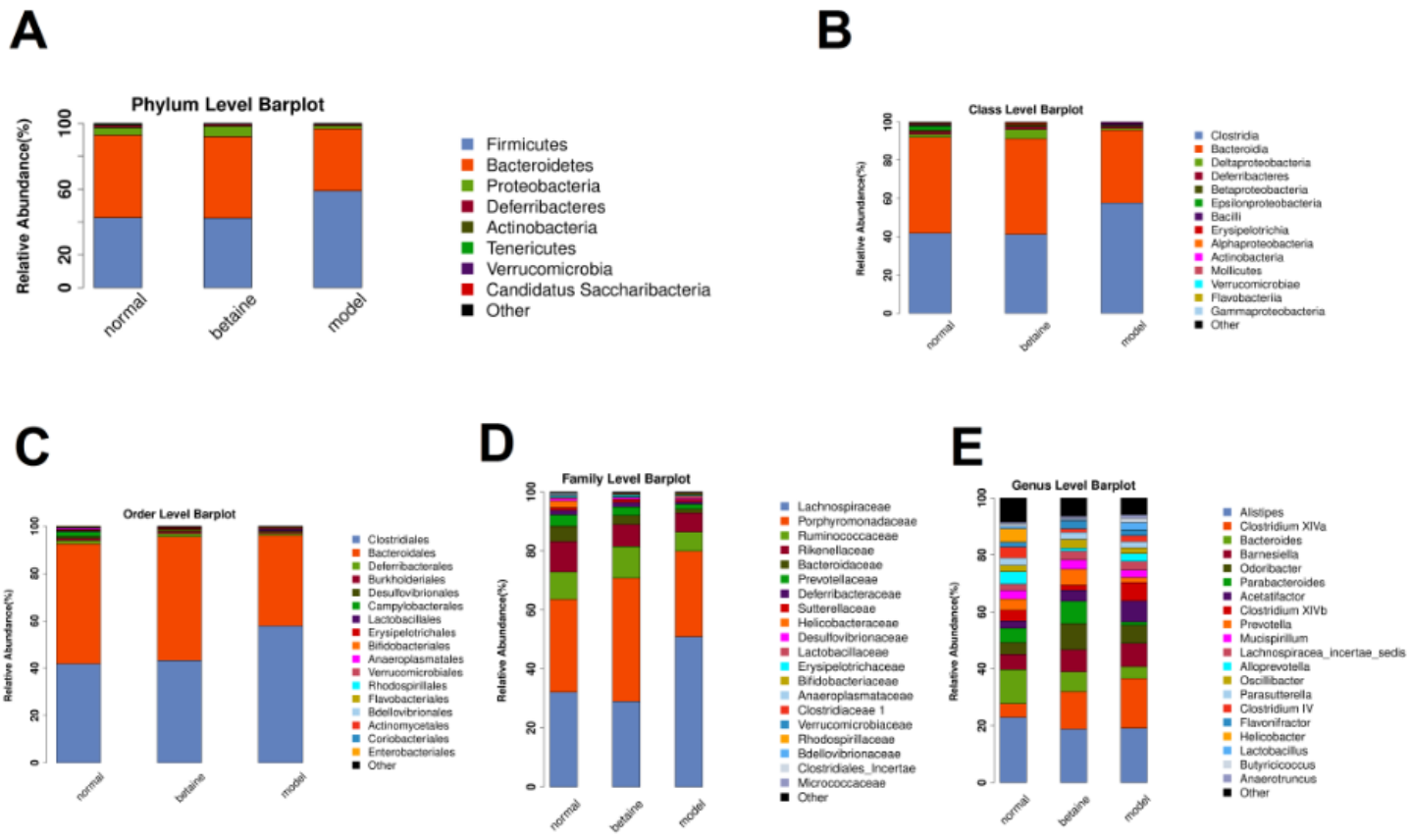

Figure 8

Species classification and abundance analysis. (A-E) The corresponding histograms of species profiling were performed on each group at the classification level of phylum, class, order, family, and genus.

Supplementary Files

This is a list of supplementary files associated with this preprint. Click to download.

- Additionalfile5.txt
- Additionalfile4.txt
- Additionalfile2.tsv
- Additionalfile6.txt
- Additionalfile1.tsv
- Additionalfile3.txt